

Inhibition Activity of Three Kind of Antibiotics for Carbon Steel Corrosion in Acetic Acid Environment

Ziwen Wang¹, Wei Bai^{1,*}, Cunying Xu², Yulu Shi¹, You Wu¹, Junming Guo¹ and Lili Feng¹

¹ Key Laboratory of Resource Clean Conversions in Ethnic Regions, Yunnan Minzu University, Kunming, 650500, PR China.

² Faculty of Metallurgical and Energy Engineering, Kunming University of Science and Technology, Kunming, 650500, PR China.

*E-mail: bw369852147@qq.com

Received: 17 August 2017 / Accepted: 22 September 2017 / Published: 12 October 2017

The inhibition mechanism of carbon steel in acetic acid medium in the presence of amoxicillin, cefaclor or cephadrine has been studied with the application of weight loss measurements, potentiodynamic polarization curves, EIS, and SEM. In order to investigate the corrosion mechanism more deeply, we characterized the frontier molecular orbital energy (E_{HOMO} , E_{LUMO}), Mulliken atomic population analysis and charge density difference by using DFT study. In the case where the spatial structure is similar in resistance, the effects of cephadrine on cephadrine and cefaclor were as follows: the inhibitory effect of cephadrine in the three drugs was the best and its inhibition rate was 87.7%. The maximum of cefaclor and amoxicillin is only 63.5% and 52.1% at the same concentration. Electrochemical test indicated that cephadrine and cefaclor behaved as cathode type inhibitors and amoxicillin behaved as mixed type inhibitor. These results of experimental and theoretical calculations were consistent and they showed that cephadrine was the most effective inhibitor.

Keywords: Antibiotic, Carbon steel, Corrosion inhibition, Acetic acid, Theoretical calculation

1. INTRODUCTION

As we all know, carbon steel is one of the widely used steel materials in many industries due to excellent mechanical properties and its low cost.[1, 2] Acetic acid as an important chemical raw material is widely used in industry process.[3-5] The electrochemical impedance spectroscopic studies indicated that the actions on cathodic surface were enhanced in the presence of acetic acid due to the reduction of un-dissociated acetic acid with a subsequent increase in the anodic current density.[6, 7] Generally, acetic acid is an organic acid that causes type of localized corrosion on carbon steel by removing the iron carbonate layer, which formed when the metal surface is exposed to an aqueous

solution.[8]Actually, highly concentrated acids which between 5 and 28 wt% are used to make serious issues to carbon steels. Furthermore, Singh M. M, who have studied the laws of acid corrosion for carbon steel, indicating that 20% (vt %) was the maximum corrosive concentration of acetic acid.[9]

Unfortunately, few researches have been published the effect of inhibitor molecular structure for carbon steel corrosion in acetic acid environment. Every year, a large number of antibiotics are discarded due to expiration[10, 11]. The biggest reason for this is that we are not aware of the environmental pollution caused by antibiotics. At the same time doctors prescribing a lot of excessive antibiotics, making antibiotics in the sale of the source can not be standardized. This is an unfair war, but we can change its results. What we can do is that as much as possible to use these wasted resources making more contributions. We hope that through the more extensive research on the failure of antibiotics, so that these antibiotics reflect their own use value once again. A large number of recovered antibiotics, so that it can be further used while protecting the environment and raise public awareness of failed antibiotics.

Organic compounds which contain N, O and S atoms are considered effective metal corrosion inhibitors.[12-16] This result is due to negatively charged organic compounds containing heterocyclic atoms (or S, Cl, O, etc.) as corrosion inhibitor forming chemical bonds which are between lone pair of compound and the atom empty track of the metal.[13, 17-19]The inhibition stability on the metal surface depends on the functional groups, aromatic, possibly by steric effect of related molecule, the electron density of donor atom, the type of corrosive environment and the nature of the interaction between π -orbital of the inhibitors and d-orbital of the iron.[20, 21]In this connection, apart from choosing acid substances as stable corrosion inhibitors in acid medium, in the molecule, suitable spatial structure and heteroatom species should also be introduced. Fortunately, structurally similar antibiotics which contain N, O, and S elements bring great convenience to study the influence of atomic species of the inhibitor pair. Amoxicillin belongs to the penicillin, while cefaclor and cephadrine belong to the cephalosporin. The three poor structure inhibitors contain within β -lactam ring and have acid resistance.[22-25]

The inhibiting mechanism is generally explained as the formation of a physically and/or chemically adsorbed film on the metal surface.[26-28]Molecular modelling with quantum chemical methods has been extensively used in the correlation of inhibitory efficiency with the molecular structure of the inhibitors.[29, 30]In order to explain the mechanism of electronic interaction between inhibitors and the metal surface, we characterize the frontier molecular orbitals (E_{HOMO} , E_{LUMO}), Mulliken population analysis and the charge density difference by first principle calculation based on density functional theory (DFT).[31, 32]

In the present work, we are mainly looked for a more clear and detailed characterization technique to show the whole reaction course of three antibiotics with the carbon steel in 20% (vt %) acetic acid. Herein, we used the characterization methods of the frontier molecular orbitals (E_{HOMO} , E_{LUMO}), Mulliken atomic population analysis and charge density difference besides electrochemical techniques, weight-loss measurements and Scanning Electron Microscopy (SEM). Moreover, all of these characterization technique illustrated that the effective of three kinds of antibiotics are in the order of cephadrine > cefaclor > amoxicillin. It is rationally and intuitively interpreted that the

dispersion of HOMO-LUMO orbits of inhibitors molecular structure determined the atoms in the reaction, mechanism and inhibition effect.

2. EXPERIMENTAL METHODS

2.1. Composition of the specimens

Preparation of the working electrode from the carbon steel having the following composition (wt %): C 0.09, Mn 0.25, Si 0.30, S 0.05, P 0.045, and Fe balance.

2.2. Medium

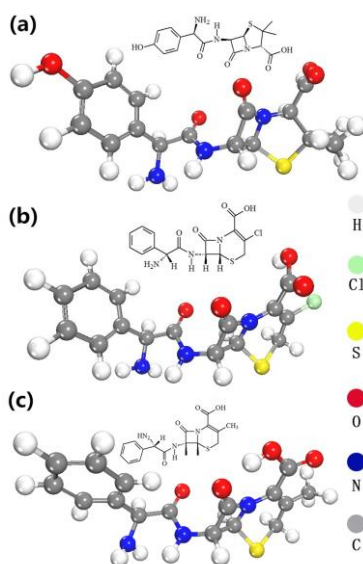


Figure 1. Inhibitor molecular structure and model of (a) amoxicillin, (b) cefaclor, (c) cefradine. The 10% gray, grass-green, yellow, red, blue and 40% gray representative the H, Cl, S, O, N and C atoms, respectively.

Acetic acid concentration of 20% (vt %) was selected as the corrosion medium (Blank). All antibiotics were known compounds and 3D chemical structures in the Fig.1.

2.3. Antibiotics IUPAC names

Amoxicillin:

(2-amino-2- (4-hydroxyphenyl) acetamido] -7-oxo-4-yl] -thia-1-azabicyclo [3.2.0] heptane-2-carboxylic acid trihydrate.

Cefaclor:

(6R, 7R) -7 - [(R) -2-amino-2-phenylacetamido] -3-chloro-8-oxo-5-thia-1-azabicyclo [4.2.0] 2-ene-2-carboxylic acid monohydrate.

Cephadrine: (7R)-7-[(2R)-2-amino-2-cyclohexa-1,4-dien-1-ylacetyl]amino}-3-methyl-8-oxo-5-thia-1-azabicyclo[4.2.0]oct-2-ene-2-carboxylic acid.

2.4. Electrochemical measurements

Type carbon steel samples in an electrochemical measurement was mechanically cut into 1cm×1cm slices, the resin-encapsulated, polished exposed surface with 100-2000 grade emery paper, washed with distilled water, skim with acetone and dried in air. Saturated calomel electrode (SCE) and a platinum electrode been used as a reference and an auxiliary electrode, respectively. In the present study, the carbon steel of the working electrode was allowed to take place after it reached a stable open circuit potential (OCP) for two hours. Potentiodynamic anode and cathode polarization curves were used a scan rate of 0.5mV/s, the scanning range was -300 ~ 300mV with respect to the stable open circuit corrosion potential. The excitation signal amplitude of AC impedance measurement was 10mV and frequency was 0.1 ~ 10⁵Hz. Analysis of impedance spectra used Zview software. Electrochemical tests were used CS350 electrochemical workstation to measuring and DKZ series electric heated water bath to constant temperature at 20°C. Potentiodynamic polarization curves and electrochemical impedance calculation as follows[33, 34]:

$$\eta_p(\%) = \left(\frac{i_{\text{corr}}^0 - i_{\text{corr}}}{i_{\text{corr}}^0} \right) \times 100 \quad (1)$$

Where i_{corr}^0 represented the current density in the absence of corrosion inhibitors and i_{corr} indicated presence inhibitors of the corrosion current density that obtained from Tafel curves.

$$\eta_{\text{EIS}}(\%) = \left(\frac{R_{\text{ct}} - R_{\text{ct}}^0}{R_{\text{ct}}^0} \right) \times 100 \quad (2)$$

Where R_{ct}^0 represented the charge transfer resistance in the absence of corrosion inhibitors and R_{ct} indicated presence inhibitors of the charge transfer resistance that obtained from the electrochemical impedance diagram.

2.5. Weight loss experiment

Type carbon steel samples in an electrochemical measurement was mechanically cut into 3cm×1cm×1cm slices and with the same composition used in the electrochemical measurements. Triplicate specimens were immersed in the 20% (vt %) acetic acid test solutions for 24 h at 20 °C in the absence and presence of amoxicillin, cefaclor and cephradine at the following concentrations: 1.0×10⁻⁵, 2.0×10⁻⁵, 5.0×10⁻⁵, 1.0×10⁻⁴ and 2.0×10⁻⁴ mol•L⁻¹.

Effect of temperature on corrosion rates has been examined. This experiment was performed in the absence and presence of 2.0×10⁻⁴ mol•L⁻¹ of amoxicillin, cefaclor and cephradine with an immersion period of 24h at 40, 60 and 80°C. In the present study, each experiment was repeated three times in the same conditions and calculated the average value using the following equation:

$$\Delta W = W_1 - W_2 \quad (3)$$

Where W_1 and W_2 are the average weight of samples before and after submersion, respectively.

The corrosion rates C_{RW} ($\text{mg}\cdot\text{cm}^{-2}\cdot\text{h}^{-1}$), the surface coverage θ and the values of inhibition efficiency η_w % obtained from gravimetric measurements were defined using the following equations [35, 36]:

$$\theta = \frac{C_{RW}^0 - C_{RW}}{C_{RW}^0} \quad (4)$$

$$C_{RW} = \frac{\Delta W}{St} = \frac{W_1 - W_2}{St} \quad (5)$$

$$\eta_w (\%) = \left(\frac{C_{RW}^0 - C_{RW}}{C_{RW}^0} \right) \times 100 \quad (6)$$

Where S is the surface area of specimen (cm^2), t is the immersion time (h), C_{RW}^0 and C_{RW} are the corrosion rates in absence and presence of inhibitors, respectively.

2.6. Scanning electron microscopy (SEM)

Four samples with the same composition used in the electrochemical measurements were immersed in 20% (vt %) acetic acid in the absence and presence of amoxicillin, cefaclor or cephadrine at 20°C for 24 hours, washed with distilled water and dry immediately. All samples examined by scanning electron microscope with an accelerating voltage of 25 kV (Holland yielding XL30 ESEM-TMP).

2.7. Theoretical calculations

All calculations were performed using the plane-wave DFT method and implemented in the Cambridge Serial Total Energy Package (CASTEP) code. [37, 38] The generalized gradient approximation (GGA) with the Perdew–Burke–Ernzerhof (PBE) formalism was used to treat the exchange–correlation effects. [39, 40] A plane wave basis set with a cut-off energy of 340 eV the Brillouin zone comprehensiveness was regulated with a $3\times 3\times 1$ k-point for geometry optimization and a $8\times 8\times 1$ k-point for electronic structure analysis. All geometry structures are fully relaxed until the convergence criteria of energy and force until the maximum atomic force are smaller than 5×10^{-6} eV/atom and 0.01 eV/Å. All complexes were performed on a 6×3 Fe atoms super cell with periodic boundary conditions and amoxicillin, cefaclor and cephadrine above the Fe atoms about 3 Å in a 20 Å vacuum, respectively.

3. RESULT AND DISCUSSION

3.1. Electrochemical experiments

3.1.1. Potentiodynamic polarization curves

The obtained potentiodynamic polarization curves for carbon steel in 20% (vt %) acetic acid which with and without of amoxicillin (a), cefaclor (b) and cephadrine (c) at concentration: 1.0×10^{-5} ,

2.0×10^{-5} , 5.0×10^{-5} , 1.0×10^{-4} and $2.0 \times 10^{-4} \text{ mol} \cdot \text{L}^{-1}$ are plotted in Fig. 2. The corrosion parameters that obtained from potentiodynamic polarization curves such as the anodic Tafel slope (b_a), cathodic Tafel slope (b_c), corrosion current density (i_{corr}), the corrosion potential (E_{corr}) and the inhibition efficiency (η_p) have been displayed in Table 1.

It can be seen from the corrosion potential (E_{corr}) in Table 1 negatively shifted between the presence and absence of cefaclor and cephradine are larger than 85 mV. This result indicates the type of the inhibitors is cathodic inhibitor. However, amoxicillin is mixed-type inhibitor with a cathodic character predominating because the value of its corrosion potential negatively shifted less than 85 mV. [41, 42] Therefore, the inhibition mechanism of the three antibiotics is to reduce the hydrogen evolution reaction on cathodic sites of mild steel. Table 1 shows that the corrosion current density (i_{corr}) decreased as the concentration of inhibitor increased and this decrease for the three kinds of antibiotics in the order of cephradine > cefaclor > amoxicillin.

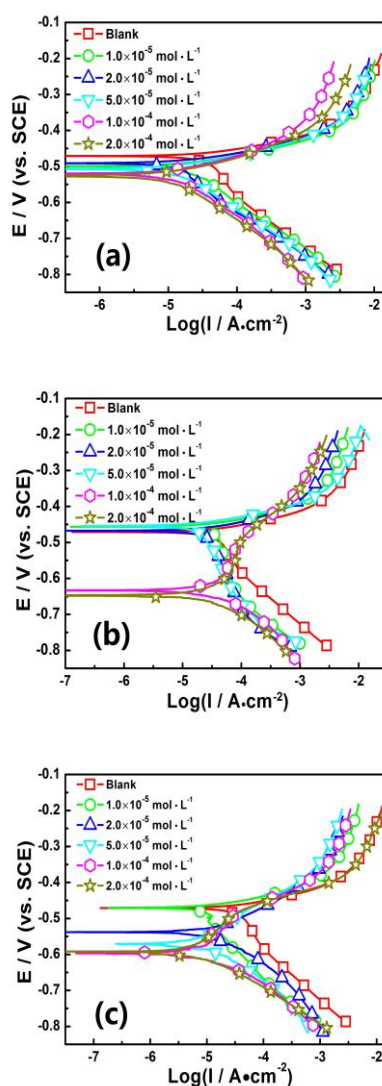


Figure 2. Polarization curves of carbon steel is immersed in 20% (vt %) acetic acid with and without of amoxicillin (a), cefaclor (b) and cephradine (c) at concentration: 1.0×10^{-5} , 2.0×10^{-5} , 5.0×10^{-5} , 1.0×10^{-4} and $2.0 \times 10^{-4} \text{ mol} \cdot \text{L}^{-1}$ liquid medium.

Table 1. Corrosion parameters of carbon steel is immersed in 20% (vt %) acetic acid with and without of amoxicillin, cefaclor and cephradine at concentration: 1.0×10^{-5} , 2.0×10^{-5} , 5.0×10^{-5} , 1.0×10^{-4} and $2.0 \times 10^{-4} \text{ mol} \cdot \text{L}^{-1}$ liquid medium.

Medium	$C/(\text{mol} \cdot \text{L}^{-1})$	$b_a/(\text{mV} \cdot \text{dec}^{-1})$	$b_c/(\text{mV} \cdot \text{dec}^{-1})$	$i_{\text{corr}}/(\mu\text{A} \cdot \text{cm}^{-2})$	E/mV	$\eta_p/(\%)$
Blank	--	29.8	-215.3	30.2	-466.4	--
Amoxicillin	1.0×10^{-5}	45.6	-134.0	19.7	-500.0	34.8
	2.0×10^{-5}	43.7	-143.9	18.2	-490.2	40.0
	5.0×10^{-5}	45.7	-122.9	13.0	-510.3	57.0
	1.0×10^{-4}	56.6	-122.1	12.9	-521.5	57.3
	2.0×10^{-4}	59.7	-125.5	11.6	-529.3	61.6
Cefaclor	1.0×10^{-5}	19.0	-126.5	19.2	-451.1	36.4
	2.0×10^{-5}	27.3	-247.1	19.1	-462.3	36.8
	5.0×10^{-5}	27.6	-293.7	17.7	-448.6	41.1
	1.0×10^{-4}	88.6	-34.0	11.0	-637.4	63.6
	2.0×10^{-4}	89.4	-36.5	10.6	-646.0	64.9
Cefradine	1.0×10^{-5}	30.0	-176.7	14.9	-476.8	50.7
	2.0×10^{-5}	66.4	-75.6	8.9	-549.9	71.2
	5.0×10^{-4}	96.8	-72.7	6.1	-568.7	79.8
	1.0×10^{-4}	125.8	-48.7	5.3	-602.9	82.5
	2.0×10^{-4}	111.4	-49.3	3.7	-597.1	87.7

Furthermore, cathodic Tafel curves resulting in parallel lines with increasing inhibitors concentration, this indicates that the addition of does not modify the hydrogen evolution mechanism.[10, 43] However, anodic current densities change quite large in the absence cefaclor (b) and cephradine (c) at concentration: 1.0×10^{-4} and $2.0 \times 10^{-4} \text{ mol} \cdot \text{L}^{-1}$, resulting in a sharp increase in Tafel slope (b_a) in the high polarization potential region. This result is attributed to the desorption process of adsorbed inhibitor on metal surface.[10, 44]

3.1.2. Electrochemical impedance spectroscopy (EIS)

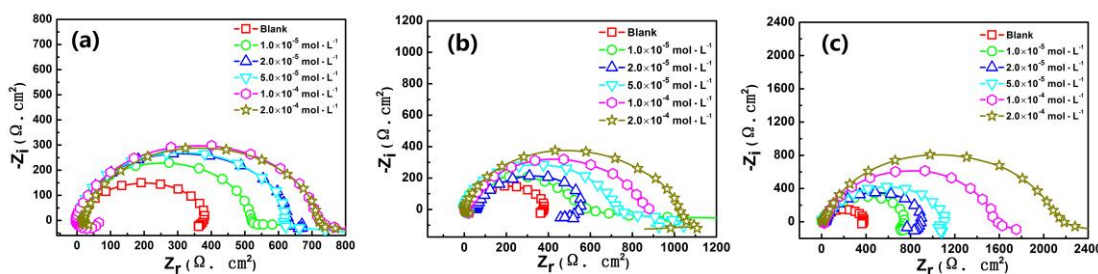


Figure 3. Nyquist plots of carbon steel is immersed in 20% (vt %) acetic acid with and without of amoxicillin (a), cefaclor (b) and cephradine (c) at concentration: 1.0×10^{-5} , 2.0×10^{-5} , 5.0×10^{-5} , 1.0×10^{-4} and $2.0 \times 10^{-4} \text{ mol} \cdot \text{L}^{-1}$ liquid medium.

In order to augment the results obtained from potentiodynamic polarization measurements, and to acquire more information about the corrosion inhibition mechanism, EIS measurements were further carried out. The Nyquist plots of carbon steel in 20% (vt %) acetic acid in the absence and presence of

amoxicillin (a), cefaclor (b) and cephradine (c) at different concentration are plotted in Fig. 3. Obviously, only one semicircle and only one time constant in the Bode plot (Fig. 4a) indicate that the reaction on the metal surface mostly controlled by charge transfer process. [45] It is clear from this figure that Nyquist plots are not perfect semicircles which have been attributed to the frequency dispersion of interfacial impedance. This result often caused by in homogeneity and roughness on the surface. [46] To get over this situation, a constant phase element (CPE) is introduced circuit instead of a pure double layer capacitor to give a more accurate fit. [47] Moreover, the constant phase element and the polarization resistance are in parallel combination and they are connected in series with the electrolyte resistance (Rs). The constant phase element is calculated by the following equation [43]:

$$Z_{CPE} = \frac{1}{Q(j\omega)^\alpha} \tag{7}$$

Where Q the magnitude of the CPE is, ω is the angular frequency, j is the imaginary number. α is the deviation parameter ($-1 \leq \alpha \leq 1$), which is commonly referred to as frequency dispersion as a result of the heterogeneity of the solid surface. [48]

The double layer capacitances, C_{dl} , for a circuit including a CPE were using the following equation [49]:

$$C_{dl} = Q(2\pi w_{max})^{\alpha-1} \tag{8}$$

Where $w_{max} = 2\pi f_{max}$ max is the frequency at the maximum value of the imaginary part of the impedance spectrum.

Table 2. The electrochemical parameters obtained from EIS plots for of carbon steel is immersed in 20% (vt %) acetic acid with and without of amoxicillin, cefaclor and cephradine at concentration: 1.0×10^{-5} , 2.0×10^{-5} , 5.0×10^{-5} , 1.0×10^{-4} and $2.0 \times 10^{-4} \text{ mol} \cdot \text{L}^{-1}$ liquid medium.

Medium	$C/(\text{mol} \cdot \text{L}^{-1})$	$R_s/(\Omega \cdot \text{cm}^2)$	α	$C_{dl}/(\mu\text{F} \cdot \text{cm}^{-2})$	$R_{ct}/(\Omega \cdot \text{cm}^2)$	$\eta_{EIS}/(\%)$
Blank	--	18.0	0.95	99.4	344.2	--
Amoxicillin	1.0×10^{-5}	16.1	0.98	53.0	503.8	31.7
	2.0×10^{-5}	10.1	0.95	63.2	591.9	41.8
	5.0×10^{-5}	10.0	0.94	71.0	626.8	45.1
	1.0×10^{-4}	16.6	0.94	69.1	641.1	46.3
	2.0×10^{-4}	18.5	0.87	82.3	718.8	52.1
Cefaclor	1.0×10^{-5}	18.0	0.98	51.7	530.6	35.1
	2.0×10^{-5}	53.1	0.83	152.0	555.8	38.1
	5.0×10^{-5}	11.5	0.91	52.3	645.0	46.6
	1.0×10^{-4}	16.4	0.82	128.0	822.3	58.1
	2.0×10^{-4}	3.3	0.87	56.4	944.0	63.5
Cefradine	1.0×10^{-5}	12.8	0.86	121.0	697.2	50.3
	2.0×10^{-5}	29.9	0.87	109.0	824.0	58.2
	5.0×10^{-5}	23.4	0.82	106.0	1035.0	66.7
	1.0×10^{-4}	18.9	0.83	142.0	1567.0	78.0
	2.0×10^{-4}	11.2	0.81	68.1	2237.0	84.6

The value of C_{dl} in Table 2 does not have a clear regularity of values in magnitude time may be due to the inhomogeneity of the film on the metal surface and the location of the corrosion occurred randomly.[50]

All EIS spectra were analyzed by the equivalent circuit in Fig. 4b, which fits well with our experimental results. In Table 2, the charge-transfer resistance (R_{ct}) decreased as the concentration of inhibitor increased and the same trend as observed in the potentiodynamic polarization results. The inhibition efficiency ($\eta_{EIS} \%$) were calculated from R_{ct} data in with and without of amoxicillin, cefaclor and cephradine getting 52.1%, 63.5% and 84.6% in the highest inhibition concentrations, respectively.

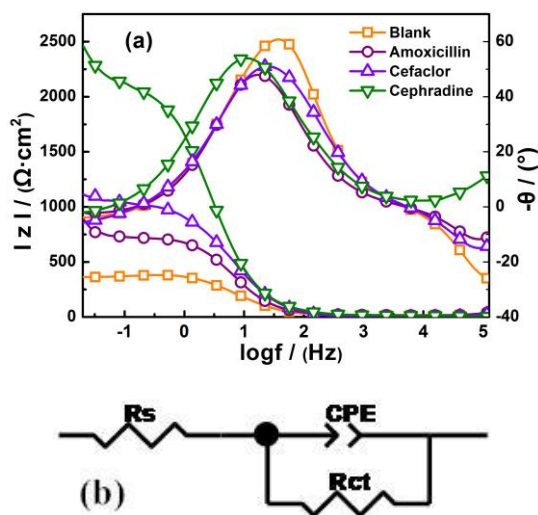


Figure 4. Bode plots of carbon steel is immersed in 20% (vt %) acetic acid absence and presence of $2.0 \times 10^{-4} \text{ mol} \cdot \text{L}^{-1}$ of amoxicillin, cefaclor and cephradine liquid medium (a). The equivalent circuit used to fit the impedance spectra which obtained from carbon steel in the experiment (b).

3.3. Gravimetric measurements

The results of the weight loss measurements for the corrosion of carbon steel in 20% (vt %) acetic acid which with and without of amoxicillin, cefaclor and cephradine at the different concentrations are offered in Table 3.

It is clear in the table that the values of inhibition efficiency ($\eta_W \%$), corrosion rate C_{RW} ($\text{mg} \cdot \text{cm}^{-2} \cdot \text{h}^{-1}$) and surface coverage θ increases with the increasing of inhibitors concentration, which shows that the three inhibitions have stabilizing effect on steel in the long time immersion. This result may be attributed to the adsorption of inhibitors on the metal surface. By observing the values of $\eta_W \%$ we found that the three kinds of antibiotics follows the order: $\eta_W \%$ (amoxicillin) $< \eta_W \%$ (cefaclor) $< \eta_W \%$ (cephradine), which shows that cephradine displays better inhibition performance compared with the other two. The data in Table 3 to the Langmuir isotherm is illustrated by plotting C/θ versus C , according to the following equations[51]:

$$\frac{C}{\theta} = \frac{1}{K_{ads}} + C \text{ (Langmuir isotherm)} \quad (9)$$

$$K_{ads} = \frac{1}{55.5} \exp\left(\frac{-\Delta G_{ads}^0}{RT}\right) \quad (10)$$

Wherein, C is the inhibitor concentration ($\text{mol}\cdot\text{L}^{-1}$), K_{ads} is the adsorption equilibrium constant, ΔG_{ads}^0 is the standard free energy of adsorption, R is the universal gas constant and T is the absolute temperature.

Table 3. Corrosion parameters obtained from weight loss measurements of carbon steel after 24h immersions in 20% (vt %) acetic acid solution with and without addition of various concentrations of amoxicillin, cefaclor and cephradine at concentration: 1.0×10^{-5} , 2.0×10^{-5} , 5.0×10^{-5} , 1.0×10^{-4} and $2.0\times 10^{-4} \text{ mol}\cdot\text{L}^{-1}$ liquid medium at 20°C .

Inhibitor	$C/$ (mol/L)	$C_{Rw}/$ ($\text{mg}\cdot\text{cm}^{-2}\cdot\text{h}^{-1}$)	θ	$\eta_w/$ (%)
blank	-	0.632	-	-
Amoxicillin	1.0×10^{-3}	0.372	41.1	41.13
	2.0×10^{-3}	0.348	45.6	45.63
	5.0×10^{-3}	0.315	50.2	50.17
	1.0×10^{-4}	0.261	58.6	58.62
	2.0×10^{-4}	0.209	67.0	67.04
Cefaclor	1.0×10^{-3}	0.339	46.3	46.31
	2.0×10^{-3}	0.327	48.1	48.09
	5.0×10^{-3}	0.305	51.7	51.66
	1.0×10^{-4}	0.250	60.4	60.43
	2.0×10^{-4}	0.195	69.2	69.18
Cephradine	1.0×10^{-3}	0.228	54.4	54.43
	2.0×10^{-3}	0.205	67.6	67.59
	5.0×10^{-3}	0.145	77.0	77.01
	1.0×10^{-4}	0.075	88.1	88.05
	2.0×10^{-4}	0.049	92.3	92.27

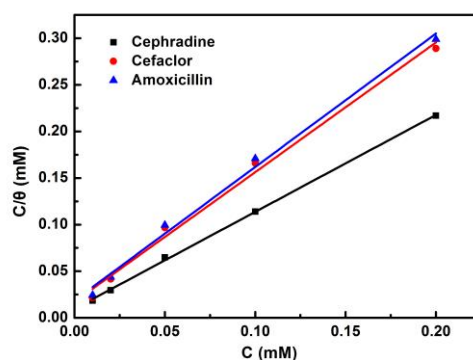


Figure 5. Langmuir adsorption isotherm in the absence and presence of $2.0\times 10^{-4} \text{ mol}\cdot\text{L}^{-1}$ of amoxicillin, cefaclor and cephradine on carbon steel samples surface in 20% (vt %) acetic acid solution.

Figure 5 displays the linear plot of the Langmuir adsorption isotherms for amoxicillin, cefaclor and cephradine with a high correlation coefficient of 0.997, 0.996 and 0.999, respectively. These results represent that the inhibitor molecules are adsorbed on the metallic surface in line with monolayer adsorption.[52]The adsorption isotherms are able to illustrate the adsorption type happening between the inhibitor molecule and metal surface.

Table 4. Thermodynamic parameters obtained from Langmuir adsorption isotherm for the 20% (vt %) acetic acid at 20°C.

Inhibitor	R ²	K _{ads}	-ΔG _{ads} /(kJ·mol ⁻¹)
Amoxicillin	0.997	53.480×10 ⁵	36.30
Cefaclor	0.996	58.140×10 ⁵	36.51
Cephradine	0.999	102.670×10 ⁵	37.89

Wherein, high value of K_{ads} implies that the inhibitor is easily and strongly adsorbed on the carbon steel surface, causing a better inhibition performance.[10]It can be seen from Table 4 that the value of K_{ads} following the order: cephradine > cefaclor > amoxicillin which explains that cephradine is the best performance among the three antibiotics. Basically, the values of ΔG_{ads} less than -20 kJ·mol⁻¹ or more positive explain that this is electrostatic force between inhibitors molecules and metal molecules. Correspondingly, the values of ΔG_{ads} around -40 kJ·mol⁻¹ or more negative are indicated that inhibitor molecules are adsorbed on the metallic surface by coordinate bond formation.[53]According to the data in Table 4 shows a mixed type adsorption phenomenon which is based on chemisorption. Obviously, chemisorption is predominant in the present study.

The effects of temperature on the corrosion of carbon steel in 20% (vt %) acetic acid solution in the 20-80°C range after 24h of immersion are presented in Table 5.

Table 5. The weight loss data in 20% (vt %) acetic acid in the absence and presence of 2.0×10⁻⁴ mol·L⁻¹ of amoxicillin, cefaclor and cephradine with an immersion period of 24h at the following temperatures: 20, 40, 60, and 80°C.

T(°C)	Without inhibitor C _{Rw} (mg·cm ⁻² ·h ⁻¹)	Amoxicillin		Cefaclor		Cephradine	
		C _{Rw} (mg·cm ⁻² ·h ⁻¹)	n(%)	C _{Rw} (mg·cm ⁻² ·h ⁻¹)	n(%)	C _{Rw} (mg·cm ⁻² ·h ⁻¹)	n(%)
20	0.0632	0.0208	67.04	0.0194	69.18	0.00486	92.3
40	0.224	0.0563	76.93	0.0493	79.80	0.0250	89.8
60	1.071	0.112	89.54	0.0951	91.12	0.0854	92.0
80	1.783	0.393	77.96	0.161	90.97	0.148	91.7

The experiments are conducted in the absence and presence of 2.0×10⁻⁴ mol·L⁻¹ of amoxicillin, cefaclor and cephradine. In weak acid media, ionization of hydrogen ions will increase as the temperature rises, resulting in higher corrosion rate of the metal. [7]It is noteworthy that the efficiency of amoxicillin first and decrease afterwards as the temperature increases (Fig.6).

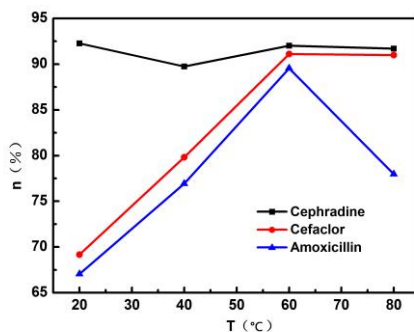


Figure 6. Variation of inhibition efficiency with temperature in 20% (vt %) acetic acid in the absence and presence of $2.0 \times 10^{-4} \text{ mol} \cdot \text{L}^{-1}$ of amoxicillin, cefaclor and cephradine with an immersion period of 24h.

This result indicated that the adsorption reaction between the inhibitor molecule and metal surface was endothermic process and the structure may be changed in the 60-80°C range while amoxicillin had acid resistance. However, the inhibition efficiency of cephradine keep almost constant with the increase in temperature. This behavior reflected the structure of cephradine is stable and the coverage of inhibitor with the metal surface not affected by temperature. Interestingly, the coverage of cefaclor reached the maximum value near 60°C which is inferred the occupancy rate of active site on metal surface saturation.

3.4. Scanning electron microscopy (SEM) analysis

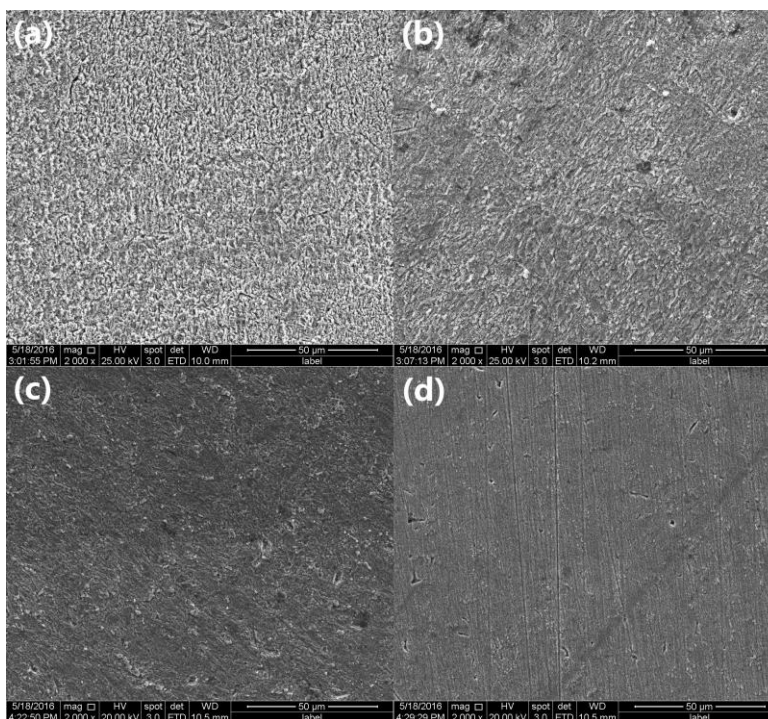


Figure 7. EMS micrographs (2000×) of carbon steel immersed in 20% (vt %) acetic acid (a) in the absence and presence of $2.0 \times 10^{-2} \text{ mol} \cdot \text{L}^{-1}$ of amoxicillin (b), cefaclor (c) and cephradine (d) 24h.

The EMS micrographs (2000 \times) of carbon steel in 20% (vt %) acetic acid (a) in the with and without of $2.0 \times 10^{-4} \text{ mol} \cdot \text{L}^{-1}$ of amoxicillin (b), cefaclor (c) and cephadrine (d) with an immersion period of 24h are displayed in Fig.7. The surface of metal surface is strongly damaged in Fig.7a, characteristic of the uniform corrosion of carbon steel in acid. In the presence of amoxicillin and cefaclor (Fig.7b and c) the damage of metal surface is slight reduced. However, deeper gully and cracks are distributed over the whole metal surface in in Fig.7b. The morphology in Fig.7d shows a smooth metal surface and even the polishing lines, which is soaked in the presence of cephadrine (Fig. 7d) in acetic acid medium. This observation clearly explains that the surface was protected by the cephadrine, which may be due to the formation of better protective films, resulting in a decrease in the attack between the metal surface and acetic acid.

3.5. Theoretical calculations

We build the model of three kinds of antibiotics systems in Fig.8 : (a) amoxicillin/Fe, (b) cefaclor/Fe, (c) cephadrine/Fe.

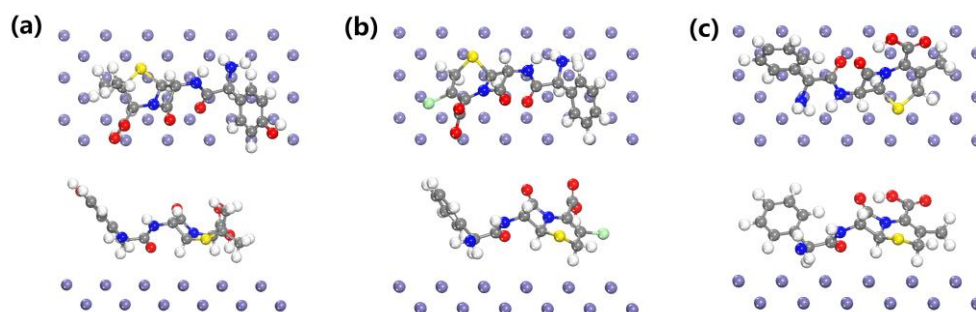


Figure 8. The simulated geometry structures of Fe combined with three kinds of antibiotics, (a) amoxicillin/Fe, (b) cefaclor/Fe, (c) cephadrine/Fe. The above is plan view, the following is front view.

3.5.1 The frontier molecular orbitals analysis

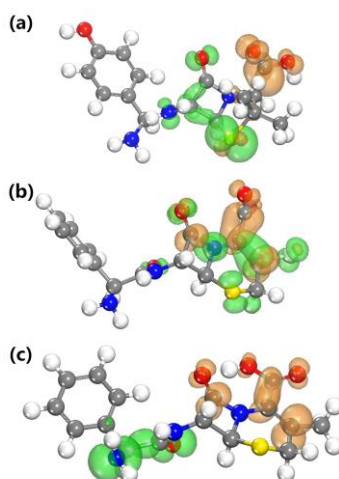


Figure 9. The HOMO-LUMO orbitals of three kinds of antibiotics, (a) amoxicillin/Fe, (b) cefaclor/Fe, (c) cephadrine/Fe.

First principle calculations based on DFT are performed to investigate the corrosion mechanism for three kinds of antibiotics and Fe (represent the steel). The frontier molecular orbitals (the highest occupied molecular orbital is HOMO and the lowest unoccupied molecular orbital is LUMO) can explain the capability of corrosion inhibition which depends on the spatial structure of molecules and distribution charges.[26] The optimized geometric configurations along with the orbitals distribution in the 3D HOMO-LUMO orbitals are presented in Fig.9. There is a certain overlap of the HOMO-LUMO orbitals of cefaclor in Fig.9b. It is revealed that electrons of cefaclor have greater possibility to occur internal transfer and the electrons transfer process may be more complexity during this reaction. In the case of Fig.9a, there is a small quantity of HOMO-LUMO orbitals in amoxicillin cause overlap. By contrast, the HOMO-LUMO orbitals of cephradine are highly fragmented and it illustrates that electrons transfer region of cephradine is straightforward (Fig.9c). The atoms that participate in the construction of HUMO-LUMO states involved in antibiotic and Fe surface reactions with a higher probability. We calculate the E_{LUMO} follow the order cephradine (3.146 eV) < cefaclor (3.381 eV) < amoxicillin (3.516 eV). These results imply that the molecular orbital has a stronger ability to accept electrons while the E_{LUMO} symbolizes is lower.[44]

3.5.2 Mulliken atomic population analysis

For the case of electron transfer with a better understanding of the comprehensive, we analyze the Mulliken atomic population analysis. W. Geng²⁷ gives a Mulliken atomic population (Q) analysis methods which is defined the charge population on a composite with the value before anchoring subtracted as ΔQ . The ΔQ (Fe) of amoxicillin/Fe, cefaclor/Fe, cephradine /Fe were 0.57, 0.32 and 0.23 respectively, which means that electronic migration direction was from Fe to antibiotics. [54]Amount of electron transfer of cephradine is the minimum. Therefore, the interaction of cephradine coupling with Fe is the best, and the degree of corrosion of internal Fe is also smallest with cephradine.

3.5.3 Charge density difference analysis

To explore the charge transfer and separation more detailed and more intuitive at the inhibitor/Fe system, the planar-averaged electron density difference as a function of position in the z-direction and the 3D charge density difference of those composites are calculated and shown in Fig.10. This can be visualized:

$$\Delta\rho = \rho_{\text{inhibitor/Fe}} - \rho_{\text{inhibitor}} - \rho_{\text{Fe}} \quad (11)$$

where $\rho_{\text{inhibitor/Fe}}$ and $\rho_{\text{inhibitor}}$ are the charge densities of the composite, the inhibitor and Fe in the same configuration, respectively. The orange and positive values indicate charge accumulation, while green and negative values represent charge depletion. Corrosion mechanism can be used to represent the electron density difference, such as the surface and internal of Fe is corroded fiercely by amoxicillin in Fig.10a. In planar-averaged drawing, the light purple and green refer to Fe and inhibitor region, respectively. More charge transfer means more serious corrosion. It is interesting to note that

the charge reappportionment mainly occur on the interface.[55] As shown in Fig. 10a, the corrosion of Fe is quite serious with amoxicillin and mainly O and S atoms involve in charges recombination. Similarly, the corrosion of Fe with cefaclor is better than amoxicillin and O and Cl atoms cause charges recombination in Fig.10b. Obviously, in Fig.10c, cephradine only gives rise to corrosion on the surface of the Fe, a very small degree of internal corrosion. Affecting charges recombination is S and N atoms. As has been mentioned above, in these donor-acceptor type interactions, HOMO orbital more involve in the reaction with Fe, whereas LUMO as active sites can restore H^+ in solvent to protect the Fe. Meanwhile, highly fragmented HOMO-LUMO orbital is a key factor in the impact of corrosion and it is expounded that cephradine has excellent corrosion resistance reasons.

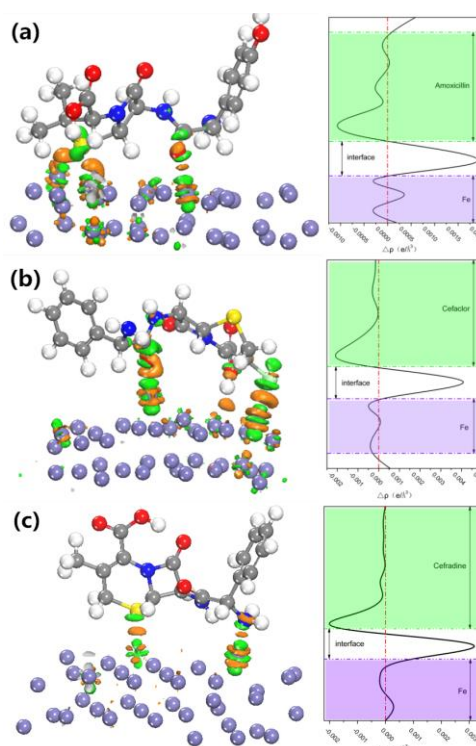


Figure 10. The charge density difference with an isovalue of 0.05 e/A³. (a)amoxicillin/Fe, (b)cefaclor/Fe, (c)cephradine/Fe.

As has been mentioned above, in these donor-acceptor type interactions, HOMO orbital more involve in the reaction with Fe, whereas LUMO as active sites can restore H^+ in solvent to protect the Fe. Meanwhile, highly fragmented HOMO-LUMO orbital is a key factor in the impact of corrosion and it is expounded that cephradine has excellent corrosion resistance reasons. By analyzing the Mulliken atomic population analysis we can find that electron gather in LUMO of inhibitors. As amoxicillin obtain electrons greater than cefaclor or cephradine, the amount of hydrogen of amoxicillin/Fe system is much larger than the other two composites. From a series of analysis shows that amoxicillin belongs to a co-existence inhibitor, cefaclor and cephradine are cathodic inhibitors. Moreover, the atoms which cause charges recombination are the reason why the HOMO-LUMO of cephradine is highly fragmented.

4. CONCLUSION

In this present research, according to the changes of anode and cathode slope and corrosion current density decreases in polarization curves, we inferred that amoxicillin was mixed-type inhibitor. Simultaneously, cefaclor and cephadrine were cathodic inhibitors. Electrochemical impedance diagrams showed the same trend as observed in the potentiodynamic polarization results. The adsorption process of cephadrine on metal surface met the Langmuir adsorption isotherm. In addition, we believed that was a co-existence adsorption process which was predominant by chemisorption. We learned through the frontier orbital analysis that LUMO orbital involvement hydrogen evolution reaction and HOMO orbital participation the reaction between inhibitor and metal. Combining charge density difference, since different atomic species involved in the reaction, cephadrine and cefaclor gained electrons less than amoxicillin so that they did not react with deep iron, protecting the metal surface and decreasing the hydrogen evolution reaction. Obviously, the results obtained by theoretical calculation explained experimental results.

ACKNOWLEDGEMENTS

This work was financially supported by Natural Science Fund Item of China(51161025, 51561032), Natural Science Fund Item of Yunnan Province(2011FZ173), Program for Innovative Research Team (in Science and Technology) in University of Yunnan Province (2011UY09), Teaching Reform Project of Yunnan Province (2013027).

References

1. S.B. Ulaeto, U.J. Ekpe, M.A. Chidiebere, E.E. Oguzie, *Int. J. M. Chem.*, 2 (2012) 158-164.
2. I. Ahamad, R. Prasad, M.A. Quraishi, *Corros. Sci.*, 52 (2010) 3033-3041.
3. E. Gulbrandsen, K. Bilkova., *Corros. Sci.*, (2006) 06364.
4. J.L. Crolet, N. Thevenot, A. Dugstad, *NACE International*.
5. Y. Sun, K. George, S. Nesic, *S. Nesic*, 03327.
6. L. Dong, C. ZhenYu, G. XingPeng, *Anti-Corros. Method. M.*, 55 (2008) 130-134.
7. G.A. Zhang, Y.F. Cheng, *Corros. Sci.*, 51 (2009) 1589-1595.
8. P.C. Okafor, S. Nesic, *Chem. Eng. Commun.*, 194 (2007) 141-157.
9. M.M. Singh, A. Gupta, *Corros.*, 56 (2000) 371-379.
10. D. Daoud, T. Douadi, H. Hamani, S. Chafaa, M. Al-Noaimi, *Corros. Sci.*, 94 (2015) 21-37.
11. R.A. Prabhu, A.V. Shanbhag, T.V. Venkatesha, *J. Appl. Electrochem.*, 37 (2007) 491-497.
12. S.K. Saha, P. Banerjee, *RSC Adv.*, 5 (2015) 71120-71130.
13. L.O. Olasunkanmi, I.B. Obot, M.M. Kabanda, E.E. Ebenso, *J. Phys. Chem. C*, 119 (2015) 16004-16019.
14. I.B. Obot, S.A. Umoren, Z.M. Gasem, R. Suleiman, B.E. Ali, *J. Ind. Eng. Chem.*, 21 (2015) 1328-1339.
15. N. Esmaeili, J. Neshati, I. Yavari, *J. Ind. Eng. Chem.*, 22 (2015) 159-163.
16. S. Hejazi, S. Mohajernia, M.H. Moayed, A. Davoodi, M. Rahimizadeh, M. Momeni, A. Eslami, A. Shiri, A. Kosari, *J. Ind. Eng. Chem.*, 25 (2015) 112-121.
17. P. Lowmunkhong, D. Ungtharak, P. Sutthivaiyakit, *Corros. Sci.*, 52 (2010) 30-36.
18. S.M. Abd El Haleem, S. Abd El Wanees, E.E. Abd El Aal, A. Farouk, *Corros. Sci.*, 68 (2013) 1-13.
19. [19] A. Döner, E.A. Şahin, G. Kardaş, O. Serindağ, *Corros. Sci.*, 66 (2013) 278-284.

20. L. C. de Sequeira Aguiar, G. M. Viana, M. V. dos Santos Romualdo, M. V. Costa, B. S. Bonato, *Lett. Org. Chem.*, 8 (2011) 540-544.
21. K.F. Khaled, *Appl. Surf. Sci.*, 256 (2010) 6753-6763.
22. A.S. Orabi, *J. Coord. Chem.*, 61 (2008) 1294-1305.
23. L.J. Lorenz, F.N. Bashore, B.A. Olsen, *J. Chromatogr. Sci.*, 30 (1992) 211-216.
24. A. Chaudhary, A. Phor, G.K. Agarwal, R.V. Singh, *Heterocycl. Commun.*, 2004, pp. 393.
25. R.B. Hamed, J.R. Gomez-Castellanos, L. Henry, C. Ducho, M.A. McDonough, C.J. Schofield, *Nat. Prod. Rep.*, 30 (2013) 21-107.
26. F. Kandemirli, S. Sagdinc, *Corros. Sci.*, 49 (2007) 2118-2130.
27. M. Lebrini, M. Lagrenée, H. Vezin, M. Traisnel, F. Bentiss, *Corros. Sci.*, 49 (2007) 2254-2269.
28. L. Larabi, O. Benali, S.M. Mekelleche, Y. Harek, *Appl. Surf. Sci.*, 253 (2006) 1371-1378.
29. W. Geng, H. Liu, X. Yao, *Phys. Chem. Chem. Phys.*, 15 (2013) 6025-6033.
30. L. Xu, W.-Q. Huang, L.-L. Wang, Z.-A. Tian, W. Hu, Y. Ma, X. Wang, A. Pan, G.-F. Huang, *Chem. Mater.*, 27 (2015) 1612-1621.
31. J.-D. Huang, S. Chai, H. Ma, B. Dong, *J. Phys. Chem. C*, 119 (2015) 33-44.
32. J. Liu, *J. Phys. Chem. C*, 119 (2015) 28417-28423.
33. R. Solmaz, *Corros. Sci.*, 79 (2014) 169-176.
34. H. Bentrach, Y. Rahali, A. Chala, *Corros. Sci.*, 82 (2014) 426-431.
35. E.E. Abd El Aal, S. Abd El Wanees, A. Farouk, S.M. Abd El Haleem, *Corros. Sci.*, 68 (2013) 14-24.
36. D.K. Yadav, M.A. Quraishi, B. Maiti, *Corros. Sci.*, 55 (2012) 254-266.
37. M.D. Segall, J.D.L. Philip, M.J. Probert, C.J. Pickard, P.J. Hasnip, S.J. Clark, M.C. Payne, *J. Phys.: Condens. Mat.*, 14 (2002) 2717.
38. H. Gao, X. Li, J. Lv, G. Liu, *J. Phys. Chem. C*, 117 (2013) 16022-16027.
39. G. Kresse, D. Joubert, *Phys. Rev. B*, 59 (1999) 1758-1775.
40. P.J. P, B. K, E. M, *Phys. Rev.*, 78 (1997) 1396.
41. M.A. Hegazy, *Corros. Sci.*, 51 (2009) 2610-2618.
42. S.K. Saha, A. Dutta, P. Ghosh, D. Sukul, P. Banerjee, *Phys. Chem. Chem. Phys.*, 17 (2015) 5679-5690.
43. B. Xu, W. Yang, Y. Liu, X. Yin, W. Gong, Y. Chen, *Corros. Sci.*, 78 (2014) 260-268.
44. X. Li, S. Deng, H. Fu, X. Xie, *Corros. Sci.*, 78 (2014) 29-42.
45. Q.B. Zhang, Y.X. Hua, *Electrochim. Acta*, 54 (2009) 1881-1887.
46. L.K. Thompson, B.S. Ramaswamy, E.A. Seymour, *Can. J. Chem.*, 55 (1977) 878-888.
47. K. Takahashi, E. Ogawa, N. Oishi, Y. Nishida, S. Kida, *Inorganica Chimica Acta*, 66 (1982) 97-103.
48. M. Hosseini, S.F.L. Mertens, M. Ghorbani, M.R. Arshadi, *Mater. Chem. Phys.*, 78 (2003) 800-808.
49. M.A. Hegazy, M. Abdallah, M.K. Awad, M. Rezk, *Corros. Sci.*, 81 (2014) 54-64.
50. D. Thirumalaikumarasamy, K. Shanmugam, V. Balasubramanian, *J. Magn. Alloy.*, 2 (2014) 36-49.
51. M. Lebrini, M. Lagrenée, H. Vezin, L. Gengembre, F. Bentiss, *Corros. Sci.*, 47 (2005) 485-505.
52. A.M. Badiea, K.N. Mohana, *Corros. Sci.*, 51 (2009) 2231-2241.
53. R. Solmaz, *Corros. Sci.*, 81 (2014) 75-84.
54. X. Zhang, Q. Chen, J. Tang, W. Hu, J. Zhang, *Sci. Rep.-UK*, 4 (2014) 4762.
55. H. Gao, B. Lu, D. Li, F. Guo, D. Dai, C. Si, G. Liu, X. Zhao, *RSC Adv.*, 6 (2016) 65315-65321